Smad7 in intestinal CD4$^+$ T cells determines autoimmunity in a spontaneous model of multiple sclerosis

Steffen Haupeltshofer[a], Teresa Leichsenring[a,1], Sarah Berg[a], Xiomara Pedreiturria[a], Stephanie C. Joachim[b], Iris Tischoff[c], Jan-Michel Otte[d], Tobias Bopp[e,f], Massimo C. Fantini[g], Charlotte Esser[h], Dieter Willbold[i,j], Ralf Gold[a], Simon Faissner[a,2], and Ingo Kleiter[a,k,2,3]

[a]St. Josef-Hospital, Department of Neurology, Ruhr-University Bochum, 44791 Bochum, Germany; [b]University Eye Clinic, Experimental Eye Research Institute, Ruhr-University Bochum, 44892 Bochum, Germany; [c]Institut für Pathologie, Bergmannsheil, 44789 Bochum, Germany; [d]Department of Internal Medicine I, Klinikum Links der Weser, 28277 Bremen, Germany; [e]Institute for Immunology, Universitätsmedizin Mainz, 55131 Mainz, Germany; [f]Research Center for Immunotherapy (FZI), Universitätsmedizin Mainz, 55131 Mainz, Germany; [g]Department of Systems Medicine, University of Rome "Tor Vergata," 00133 Roma RM, Italy; [h]Leibniz-Institut für Umweltmedizinische Forschung, Heinrich Heine University Düsseldorf, 40225 Düsseldorf, Germany; [i]Institut für Physikalische Biologie, Heinrich Heine University Düsseldorf, 40225 Düsseldorf, Germany; [j]Institute of Complex Systems (ICS-6), Forschungszentrum Jülich, 52425 Jülich, Germany; and [k]Marianne-Strauss-Klinik, Behandlungszentrum Kempfenhausen für Multiple Sklerose Kranke gGmbH, 82335 Berg, Germany

Edited by David A. Hafler, Yale University School of Medicine, New Haven, CT, and accepted by Editorial Board Member Peter Cresswell November 4, 2019 (received for review April 12, 2019)

Environmental triggers acting at the intestinal barrier are thought to contribute to the initiation of autoimmune disorders. The transforming growth factor beta inhibitor Smad7 determines the phenotype of CD4$^+$ T cells. We hypothesized that Smad7 in intestinal CD4$^+$ T cells controls initiation of opticospinal encephalomyelitis (OSE), a murine model of multiple sclerosis (MS), depending on the presence of gut microbiota. Smad7 was overexpressed or deleted in OSE CD4$^+$ T cells to determine the effect on clinical progression, T cell differentiation, and T cell migration from the intestine to the central nervous system (CNS). Smad7 overexpression worsened the clinical course of OSE and increased CNS inflammation and demyelination. It favored expansion of intestinal CD4$^+$ T cells toward an inflammatory phenotype and migration of intestinal CD4$^+$ T cells to the CNS. Intestinal biopsies from MS patients revealed decreased transforming growth factor beta signaling with a shift toward inflammatory T cell subtypes. Smad7 in intestinal T cells might represent a valuable therapeutic target for MS to achieve immunologic tolerance in the intestine and suppress CNS inflammation.

TGF-beta | T helper cell | multiple sclerosis | gut–brain axis | Smad7

The intestinal barrier has emerged as an important player in balancing health and disease in several autoimmune disorders (1). Changing the extent and composition of the intestinal microbiota turned out to be a mechanism influencing the outcome of experimental models of multiple sclerosis (MS) (2, 3). MS is a challenging and frequently occurring neurological disorder with no curative treatment available (4). Knowledge about the immunopathogenesis of MS has increased tremendously; however, mechanisms leading to initiation of autoimmunity are still elusive (5). The activation and polarization of autoreactive CD4$^+$ T cells at barrier organs such as the skin, lung, and intestine are thought to trigger various autoimmune diseases and might represent a valuable treatment target in MS (6–9).

The cytokine transforming growth factor beta (TGF-β) and its inhibitor Smad7 control the differentiation of naïve CD4$^+$ T cells into different subtypes (10, 11). Phosphorylation of receptor-associated Smad proteins drives the signal transduction from the TGF-β receptor (TGF-βR) to the nucleus (11). TGF-β signaling regulates itself in a negative feedback loop by induction of inhibitory Smad7, which ubiquitinates the TGF-βRI and prevents the phosphorylation of Smad proteins, thereby blocking TGF-β signaling (11). Thus, Smad7 is responsible for the fine-tuning of TGF-β signals. TGF-β signaling leads to enhanced induction of regulatory T (Treg) cells, which are characterized by low or absent Smad7 expression (12). The additional presence of interleukin (IL) 6 and IL-23 in the cytokine milieu during differentiation results in polarization toward T helper (Th) 17 cells (13, 14).

Significance

Mechanisms leading to initiation of the autoimmune disorder multiple sclerosis (MS) are still elusive. Environmental triggers acting at barrier organs such as the intestine could contribute to local activation of autoreactive lymphocytes and consecutive migration to the CNS. Here, we demonstrate that overexpression of the TGF-beta inhibitor Smad7 in intestinal CD4$^+$ T cells of mice lowered the threshold for autoimmunity and favored expansion and migration of inflammatory T cells. In contrast, specific deletion of Smad7 in CD4$^+$ T cells mediated protection toward development of autoimmunity via regulatory CD4$^+$ T cell differentiation and anergy. A dysregulation of TGF-beta/Smad7 signaling was also found in intestinal biopsies from MS patients, indicating a contribution of the intestinal barrier in the immunopathology of MS.

Author contributions: S.H., S.F., and I.K. designed research; S.H., T.L., S.B., X.P., I.T., and I.K. performed research; S.C.J., J.-M.O., T.B., and M.C.F. contributed new reagents/analytic tools; S.H., T.L., S.B., X.P., I.T., S.F., and I.K. analyzed data; and S.H., S.C.J., C.E., D.W., R.G., S.F., and I.K. wrote the paper.

Competing interest statement: S.C.J. received travel funding and/or speaker honoraria from Bayer, Novartis, and Roche; and received research support from Bayer, Novartis, Roche, and Ursapharm; all unrelated to the content of this manuscript. T.B. received speaker honoraria from Biogen, Novartis, and Roche; and is a member of the advisory board for Immunology of Novartis; all unrelated to the content of this manuscript. R.G. received speaker and board honoraria from Baxter, Bayer Schering, Biogen Idec, CLB Behring, Genzyme, Merck Serono, Novartis, Stendhal, Talecris, and TEVA; and his department received grant support from Bayer Schering, Biogen Idec, Genzyme, Merck Serono, Novartis, and TEVA; all unrelated to the content of this manuscript. S.F. received travel grants from Biogen Idec and Genzyme; speaker or board honoraria from Novartis and Celgene; and research support from Novartis; all unrelated to the content of this manuscript. I.K. has received speaker honoraria and travel funding from Bayer, Biogen, Novartis, Merck, Sanofi Genzyme, and Roche; speaker honoraria from Mylan; travel funding from the Guthy-Jackson Charitable Foundation; consulted for Alexion, Bayer, Biogen, Chugai, IQVIA, Novartis, Merck, and Roche; and received research support from Chugai and Diamed; all unrelated to the content of this manuscript.

This article is a PNAS Direct Submission. D.A.H. is a guest editor invited by the Editorial Board.

[1]Present address: Neurologische Klinik, REGIOMED Klinikum Coburg, 96450 Coburg, Germany.

[2]S.F. and I.K. contributed equally to this work.

[3]To whom correspondence may be addressed. Email: ingo.kleiter@rub.de.

This article contains supporting information online at https://www.pnas.org/lookup/suppl/doi:10.1073/pnas.1905955116/-/DCSupplemental.

First published December 3, 2019.

Up-regulation of Smad7 favors Th1 and Th2 differentiation by inhibiting TGF-β signaling and allowing expression of T-bet or GATA-3, respectively (15, 16). Increased expression of Smad7 at the intestinal barrier is involved in the pathogenesis of inflammatory bowel diseases (17). Local inhibition of Smad7 successfully restored immune homeostasis and alleviated clinical symptoms in patients with Crohn's disease (18).

The intestinal compartment influences the central nervous system (CNS) through physiological contributions of the microbiota, modulation of intestinal barrier function, and afferent signaling transmitted through the enteric nervous system and peripheral nerves (19, 20). Occurrence of antigens and peptides provided by nutrients and pathogens can induce inflammation, which appears particularly relevant in MS pathogenesis (21, 22). Immune cells residing in the gut contribute to the maintenance of tolerance. Suppressive immune cells including intestinal dendritic cells (DCs), FoxP3$^+$ Treg cells, and intraepithelial lymphocytes (IELs) are able to secrete high amounts of TGF-β and IL-10, preventing CD4$^+$ T cells from achieving inflammatory properties in the intestine (23).

In this study, we investigated the role of intestinal CD4$^+$ T cells for the initiation of CNS autoimmunity using the mouse model opticospinal encephalomyelitis (OSE), which spontaneously develops demyelinating lesions in the spinal cord and optic nerves (24, 25). Results were corroborated in humans by examining T cell differentiation in intestinal biopsies of MS patients. Based on our study, we postulate that the expression level of Smad7 in intestinal CD4$^+$ T cells determines immunological tolerance at the mucosal barrier and thereby controls CNS autoimmunity.

Methods

Animals. The transgenic mouse strains TCR^{MOG} (2D2) (26), IgH^{MOG} (TH) (27), CD2-Smad7 (Smad7^{CD2}) (28), CD4Cre-Smad7$^{fl/fl}$ (Smad7$^{CD4-/-}$) (10), THxSmad7^{CD2}, THxSmad7$^{CD4-/-}$, 2D2xSmad7^{CD2}, 2D2xSmad7$^{CD4-/-}$, 2D2xTH (=OSE), 2D2xTHxSmad7^{CD2} (=Smad7^{CD2}-OSE), 2D2xTHxSmad7$^{CD4-/-}$ (=Smad7$^{CD4-/-}$-OSE), and 2D2xNur77 (29), all on a C57BL/6 genetic background, and C57BL/6 control mice were bred in the animal facility of the Center for Clinical Research (Zentrum für Klinische Forschung I; Zentrale Tierversuchsanstalt der Medizin) at the Ruhr-University Bochum under environmentally controlled specific pathogen-free conditions with free access to food and water.

Induction of Spontaneous Opticospinal Encephalomyelitis and Experimental Autoimmune Encephalomyelitis. OSE mice develop spontaneous clinical symptoms after ∼28 d and were scored and weighed daily for 80 d after birth. If not otherwise specified, both healthy and diseased OSE mice were used for histology, FACS analysis, and cell-culture experiments (Table 1). For induction of experimental autoimmune encephalomyelitis (EAE), 6- to 8-wk-old female wild-type C57BL/6 mice were immunized with 50 μg MOG$_{35-55}$ solved in PBS and complete Freund's adjuvant as described previously (30). Mice were injected with 200 ng pertussis toxin (PTX) on days 0 and 2 to ensure blood–brain barrier permeabilization. Animals were scored daily as described above and killed after 20 d at the peak of disease.

Establishment of the Adoptive Transfer Model. For the adoptive transfer of autoantigen-specific T cells, EAE was induced as described above. After 30 d, CD4$^+$ T cells were isolated from either the intestine, spleen, or lymph nodes from respective EAE donor mice or OSE mice. We injected 1×10^6 isolated CD4$^+$ T cells into recipient mice of various genotypes as indicated. Mice did not receive irradiation prior to adoptive transfer (31, 32). PTX was injected in the indicated experiments.

Eradication of Gut Microbiota and α4β7 Inhibition. For eradication of gut microbiota, the antibiotics ampicillin (1 g/mL), vancomycin (0.5 g/mL), neomycinsulfat (1 g/mL), and metronidazole (1 g/mL) were given by oral gavage every second day during AT (33). For therapeutic eradication, antibiotics were given when first clinical symptoms appeared. Prophylactic eradication was performed 5 d before predicted disease initiation. TR-14035 (MedChemExpress) was injected daily for 20 d at 10 μM (34) to inhibit α4β7 surface expression on T cells and to reduce T cell migration to the intestine.

Selection of Human Intestinal Biopsies. Twenty-seven patients with MS, who underwent colonoscopy with intestinal biopsy between 2004 and 2015, were identified retrospectively. Twenty-seven control subjects, not diagnosed with a chronic inflammatory disease of the CNS, were matched to MS patients regarding gender and age (for patient characteristics, see *SI Appendix*, Fig. S7 and Table S1).

Statistical Analysis. All statistical tests were performed with GraphPad Prism 6.0 software. Clinical disease courses were analyzed measuring the area under the curve (AUC) following a Mann–Whitney *U* test. Experiments with 3 or more groups were analyzed using 2-way ANOVA, followed by Tukey post hoc test. Human intestinal biopsies were compared with Student's *t* test in case data were normally distributed and Mann–Whitney *U* test in case data were not normally distributed. A P value < 0.05 was considered statistically significant.

Study Approval. All experiments that involved animals were approved by and performed in compliance with guidelines of the animal care committee of the authorities of North Rhine Westphalia (Landesamt für Natur, Umwelt und Verbraucherschutz Nordrhein-Westfalen; file no. 84-02.04.2016.A062). Analysis of human samples was approved by the institutional ethics review board of the Medical Faculty of Ruhr-University Bochum (file no. 4747-13). All patients were contacted and informed about this retrospective study and gave their written informed consent for the use of their tissue samples for scientific analysis.

Data Availability. All data are included in the manuscript and *SI Appendix*.

Results

The Expression Level of Smad7 in CD4$^+$ T Cells Determines the Outcome of Spontaneous Autoimmune Encephalomyelitis. To evaluate whether Smad7 in CD4$^+$ T cells sets the threshold for initiation of spontaneous autoimmune demyelination, mice transgenic for MOG$_{35-55}$–recognizing T and B cell receptors (OSE mice) (24, 25) were crossed with mice with T cell-specific Smad7 overexpression (Smad7^{CD2}-OSE) or CD4$^+$-specific Smad7 deletion (Smad7$^{CD4-/-}$-OSE), respectively. Specific Smad7 overexpression or deletion in CD4$^+$ and CD8$^+$ T cells, but not in CD19$^+$ B cells, was confirmed by RT-PCR (*SI Appendix*, Fig. S1*A*).

Clinical disease in OSE mice developed after approximately 1 mo. OSE mice had a mean clinical score of 1.5 ± 0.3 and a disease incidence of 47% after 80 d (Fig. 1 *A* and *B* and Table 1). Mice with Smad7 overexpression in T cells had a significantly increased mean score of 3.5 ± 0.8, increased disease incidence of 83%,

Table 1. Incidence of spontaneous encephalomyelitis in OSE, Smad7^{CD2}-OSE, and Smad7$^{CD4-/-}$-OSE

Mice	Disease incidence (%)		Mean score		Mean day of onset		Maximum score		OSE-related death (%)
OSE	28/57 (47)		1.5 ± 0.37		28.4 ± 0.6		1.7 ± 1.9		0/57 (0)
Smad7^{CD2}-OSE	38/46 (83)	$P = 0.008$	3.5 ± 0.78	$P = 0.008$	23.7 ± 1.2	$P = 0.001$	3.1 ± 0.8	$P = 0.004$	8/46 (17)
Smad7$^{CD4-/-}$-OSE	3/34 (8)	$P = 0.034$	0.2 ± 0.94	$P = 0.034$	35.2 ± 5.7	$P = 0.002$	0.3 ± 0.2	$P = 0.017$	0/34 (0)

Incidence of opticospinal encephalomyelitis (OSE) was monitored for 80 d after birth. Disease incidence, mean score, mean day of onset, maximum score, and OSE-related deaths (animals with a score >7 were excluded due to experimental animal guidelines) are reported as the number of mice affected/total number of mice. Evaluated mouse strains are OSE, Smad7^{CD2}-OSE, and Smad7$^{CD4-/-}$-OSE. Data are shown as mean ± SEM. Smad7^{CD2}-OSE and Smad7$^{CD4-/-}$-OSE were compared with OSE mice. Statistical analysis of the disease incidence was performed by AUC and a Mann–Whitney *U* test. The statistical analyses for mean score, mean day of onset, maximum score, and OSE-related deaths were performed using a 2-way ANOVA with a Tukey post hoc test.

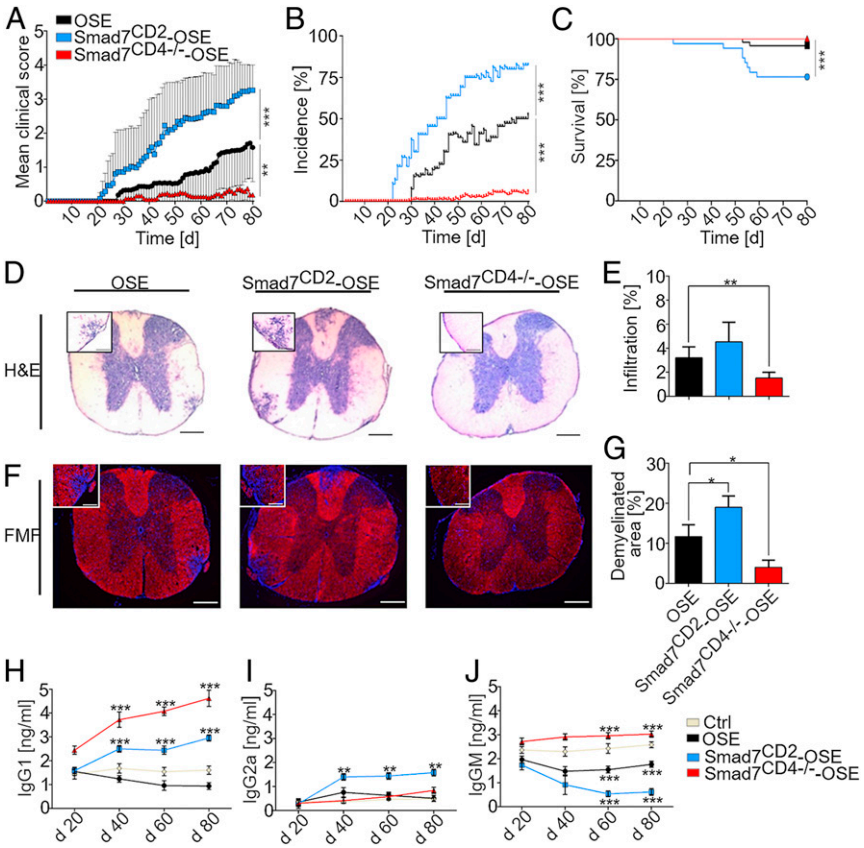

Fig. 1. Smad7 deletion in T cells reduces severity and incidence of opticospinal encephalomyelitis. (*A–C*) Clinical score (*A*), disease incidence (*B*), and survival analysis (*C*) for 2D2xTH (OSE) mice with a deletion of Smad7 in T cells (Smad7$^{CD4-/-}$-OSE, $n = 34$), compared with mice with an overexpression of Smad7 in T cells (Smad7^{CD2}-OSE, $n = 46$) and control mice (OSE, $n = 57$), starting at the day of birth and followed for 80 d after birth. (*D–G*) Histology obtained at day 80 after birth shows representative slices from the thoracic parts of the spinal cord with hematoxylin and eosin (H&E) staining (*D*), myelin staining with FluoroMyelin F (FMF) (*F*), and quantification of cell infiltration (*E*) and demyelination (*G*) ($n = 12$ mice per group). Stainings were done for adjacent slices. (*D* and *F*, *Insets*) Close-up images of infiltrated areas. (Scale bars, 250 and 100 μm [*Insets*].) (*H–J*) Analysis of immunoglobulins IgG1 (*H*), IgG2a (*I*), and IgM (*J*) obtained from blood at day 20, 40, 60, and 80 after birth ($n = 24$ mice each group). For statistical analysis of the clinical disease course, area under the curve and Mann–Whitney *U* test were done (*A–C*). Analysis for areas of infiltration (*E*) and demyelination (*G*) was performed using 2-way ANOVA with Tukey post hoc test. Ig values (*H–J*) were analyzed using 2-way ANOVA and Šidák post hoc test. Data are shown as mean ± SD (*A*) or mean ± SEM (*E* and *G–J*). Data were compared with normal OSE mice as a control (*A–G*) or with wild-type mice (*H–J*), respectively. $^{*}P < 0.05$, $^{**}P < 0.01$, $^{***}P < 0.001$.

and increased disease-related mortality (8/46 mice), whereas no OSE-related deaths occurred in the other groups (Fig. 1*C*). Mice with a CD4^{+} T cell-specific Smad7 deletion had a mean score of 0.2 ± 0.9 with a disease incidence of 8%. Histological analysis revealed increased inflammation in the spinal cord (Fig. 1 *D* and *E*) and more demyelination (Fig. 1 *F* and *G*) in Smad7^{CD2}-OSE compared with Smad7$^{CD4-/-}$-OSE mice. On the contrary, mice with a CD4^{+} T cell-specific Smad7 deletion showed significantly less infiltration and demyelination in the spinal cord compared with OSE and Smad7^{CD2}-OSE mice.

Examination of the T helper cell subsets Th1 (CD4^{+}IFN-γ^{+}), Th17 (CD4^{+}IL-17^{+}), and Treg (CD4^{+}FoxP3^{+}) in the spleen of Smad7^{CD2}-OSE mice revealed unchanged frequencies of Th1 cells and showed a significant reduction of Th17 frequencies compared with OSE (*SI Appendix*, Fig. S1*B*). Th1 CD4^{+} T cells were significantly decreased in Smad7$^{CD4-/-}$-OSE compared with OSE mice. Treg frequencies were unaltered in all groups. Evaluation of mesenteric lymph node cells revealed reduced frequencies of Th1 cells in Smad7$^{CD4-/-}$-OSE, while OSE and Smad7^{CD2}-OSE mice had comparable amounts of Th1 cells (*SI Appendix*, Fig. S1*C*). The frequency of Tregs was slightly elevated in Smad7$^{CD4-/-}$-OSE compared with OSE mice (*SI Appendix*, Fig. S1*C*). In axillary lymph nodes, frequencies of T cell subsets were unchanged between OSE, Smad7^{CD2}-OSE, and Smad7$^{CD4-/-}$-OSE mice (*SI Appendix*, Fig. S1*D*). In the Peyer's patches (PPs) of the small intestine, low numbers of Th1 and Th17 cells were found in OSE, Smad7^{CD2}-OSE, and Smad7$^{CD4-/-}$-OSE mice. However, Tregs were increased in the PPs of Smad7$^{CD4-/-}$-OSE mice (*SI Appendix*, Fig. S1*E*). B220^{+} B cells were the dominant cell type in PPs which were, interestingly, reduced in Smad7$^{CD4-/-}$-OSE mice (*SI Appendix*, Fig. S1*F*).

We then investigated whether Smad7 manipulation in CD4^{+} T cells also alters CNS inflammation and measured levels of the cytokines interferon (IFN)-γ, IL-17, and IL-10 in the CNS. We found that IFN-γ levels were slightly higher in Smad7^{CD2}-OSE and significantly decreased in Smad7$^{CD4-/-}$-OSE mice compared with OSE mice (*SI Appendix*, Fig. S1*G*). IL-17 concentration was not different in OSE compared with Smad7^{CD2}-OSE mice; however, IL-17 was significantly decreased in Smad7$^{CD4-/-}$-OSE compared with OSE mice (*SI Appendix*, Fig. S1*H*). IL-10 levels were unchanged in all 3 groups (*SI Appendix*, Fig. S1*I*). Cell numbers of respective organs did not differ, indicating that the observed changes in T helper frequencies were not influenced by differing cell numbers (*SI Appendix*, Table S2).

Quantification of serum immunoglobulins (Igs) at days 20, 40, 60, and 80 after birth revealed a time-dependent increase of IgG1 in Smad7^{CD2}-OSE and Smad7$^{CD4-/-}$-OSE mice, whereas IgG1 remained unchanged in OSE and in wild-type control mice

(Fig. 1*H*). IgG2a doubled from day 40 in Smad7^{CD2}-OSE mice and IgM decreased in Smad7^{CD2}-OSE and OSE and slightly increased in Smad7$^{CD4-/-}$-OSE mice over time (Fig. 1 *I* and *J*).

Smad7 Overexpression in T Cells Leads to Structural Changes and an Altered T Lymphocyte Composition of the Intestinal Mucosa. To examine whether the increased severity of clinical disease in Smad7^{CD2}-OSE mice was associated with alterations of the gut mucosa, we investigated the architecture of the small and large intestine (*SI Appendix*, Fig. S2 *A* and *B*). The submucosa of the jejunum and colon was thicker in OSE and Smad7^{CD2}-OSE compared with control mice (*SI Appendix*, Fig. S2*C*). Lamina propria (LP), stratum circulare, and stratum longitudinale did not differ; there were only minor changes in the depth of the crypts (*SI Appendix*, Fig. S2 *D*–*G*).

As pathogenesis of OSE involves an interaction of the microbial colonization of the intestine with the immune system, we investigated whether the inflammatory phenotype in Smad7^{CD2}-OSE was associated with an altered CD4$^+$ T cell composition in the intestine. Amounts of CD4$^+$ T cells in the LP of the small and large intestine were unaltered (Fig. 2*A*) but frequencies of the CD4$^+$ T cell subsets Th1, Th17, and Treg differed (Fig. 2*B* and *SI Appendix*, Fig. S2*H*). In detail, inflammatory Th1 cells were increased in the LP of Smad7^{CD2}-OSE mice, whereas Smad7$^{CD4-/-}$-OSE mice had fewer Th1 lymphocytes. Th17 frequencies were decreased in both Smad7^{CD2}-OSE and Smad7$^{CD4-/-}$-OSE compared with OSE mice. On the contrary, Treg frequencies were higher in the LP of Smad7$^{CD4-/-}$-OSE mice. Despite increased numbers of inflammatory Th1 cells in the LP of Smad7^{CD2}-OSE mice, inflammation in the intestinal compartments was absent.

To identify the site of T cell subtype accumulation in the intestine, we compared CD4$^+$ T cell subsets in the duodenum, jejunum, ileum, and colon. Th1 frequencies did not differ between Smad7$^{CD4-/-}$-OSE and OSE mice in the intestinal compartments; however, they were significantly elevated in Smad7^{CD2}-OSE mice in the jejunum and ileum (Fig. 2*C* and *SI Appendix*, Fig. S2*I*). The amount of Th17 cells in the intestine of Smad7^{CD2}-OSE mice was significantly decreased in the jejunum and ileum, whereas no changes were found in Smad7$^{CD4-/-}$-OSE mice (Fig. 2*D*). For Treg frequencies, we found a slight but not significant increase of Tregs in all parts of the intestine in Smad7$^{CD4-/-}$-OSE compared with OSE mice (Fig. 2*E*). Histological staining of the small intestine revealed elevated levels of Smad7$^+$ cells in Smad7^{CD2}-OSE mice compared with OSE and Smad7$^{CD4-/-}$-OSE mice (Fig. 2*F*). Collectively, these data indicate that the expression level of Smad7 influences the amount and differentiation of T cells in the intestine.

Smad7 Overexpression in CD4$^+$ T Cells Causes Autoreactive Activation in the Intestine. To address whether Smad7 in CD4$^+$ T cells might be involved in the process of overcoming the tolerogenic milieu and determine the increased susceptibility to autoimmune CNS inflammation in Smad7^{CD2}-OSE mice, we quantified to what extent CD4$^+$ T cell proliferation can be induced upon antigen stimulation. The frequency of MOG$_{35–55}$–specific lymphocytes obtained from the intestinal LP did not differ between OSE, Smad7^{CD2}-OSE, and Smad7$^{CD4-/-}$-OSE mice (*SI Appendix*, Fig. S3*A*).

T cells derived from the spleen of Smad7^{CD2}-OSE showed enhanced proliferative potential ex vivo upon stimulation with MOG$_{35–55}$ peptide and with recombinant full-length myelin oligodendrocyte glycoprotein (rMOG) protein compared with T cells derived from OSE and Smad7$^{CD4-/-}$-OSE mice (*SI Appendix*, Fig. S3*B*). CD4$^+$ T cells from the small intestine of Smad7^{CD2}-OSE mice showed enhanced proliferative potential upon restimulation compared with intestinal CD4$^+$ T cells from OSE and Smad7$^{CD4-/-}$-OSE mice (Fig. 3 *A* and *B*). CD4$^+$ T cells

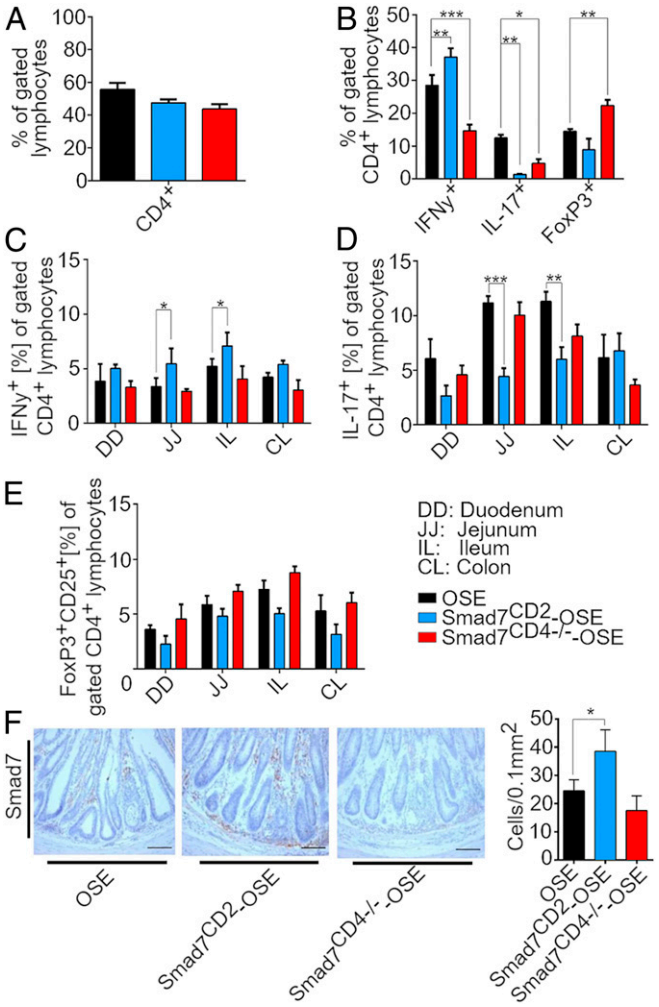

Fig. 2. Smad7 expression in T cells determines intestinal T cell differentiation and influences architecture of the gut submucosa. (*A*) Investigation of CD4$^+$ T cell frequencies from the lamina propria of 80-d-old OSE, Smad7^{CD2}-OSE, or Smad7$^{CD4-/-}$-OSE mice (n = 12 mice each group). (*B*) Flow cytometric frequency analysis of lamina propria-derived Th1, Th17, and Treg cell subtypes (n = 12 mice each group). (*C*–*E*) Flow cytometric analysis of Th1, Th17, and Treg frequencies in the duodenum, jejunum, ileum, and colon (n = 6 mice each group). (*F*) Staining of the small intestine for H&E and Smad7 using DAB and quantification of Smad7$^+$ cells. Statistical analyses were performed using 2-way ANOVA with Tukey post hoc test. T cell frequencies of Smad7 expression were compared with OSE mice. Results are shown as mean ± SEM. $^*P < 0.05$, $^{**}P < 0.01$, $^{***}P < 0.001$.

derived from the large intestine showed the same behavior but overall a much lower potential to proliferate (Fig. 3*C*).

Mixed lymphocyte reactions revealed that intestine-derived Tregs, and to a lesser degree DCs, both obtained from wild-type mice, were not able to reduce proliferation of lymph node-derived Smad7^{CD2}-OSE T cells upon MOG restimulation (Fig. 3 *D* and *E*). In contrast, much smaller numbers of tolerance-inducing cells were sufficient to suppress proliferation of lymph node-derived Smad7$^{CD4-/-}$-OSE T cells.

To evaluate proliferation of CD4$^+$ T cells in vivo, we applied bromodeoxyuridine (BrdU) to mice and performed histological analyses of T cell proliferation within the LP 24 h after application. We found significantly less T cell proliferation in Smad7$^{CD4-/-}$-OSE compared with OSE and Smad7^{CD2}-OSE mice (Fig. 3 *F* and *G*). The total cell number did not differ between different genotypes (*SI Appendix*, Table S2).

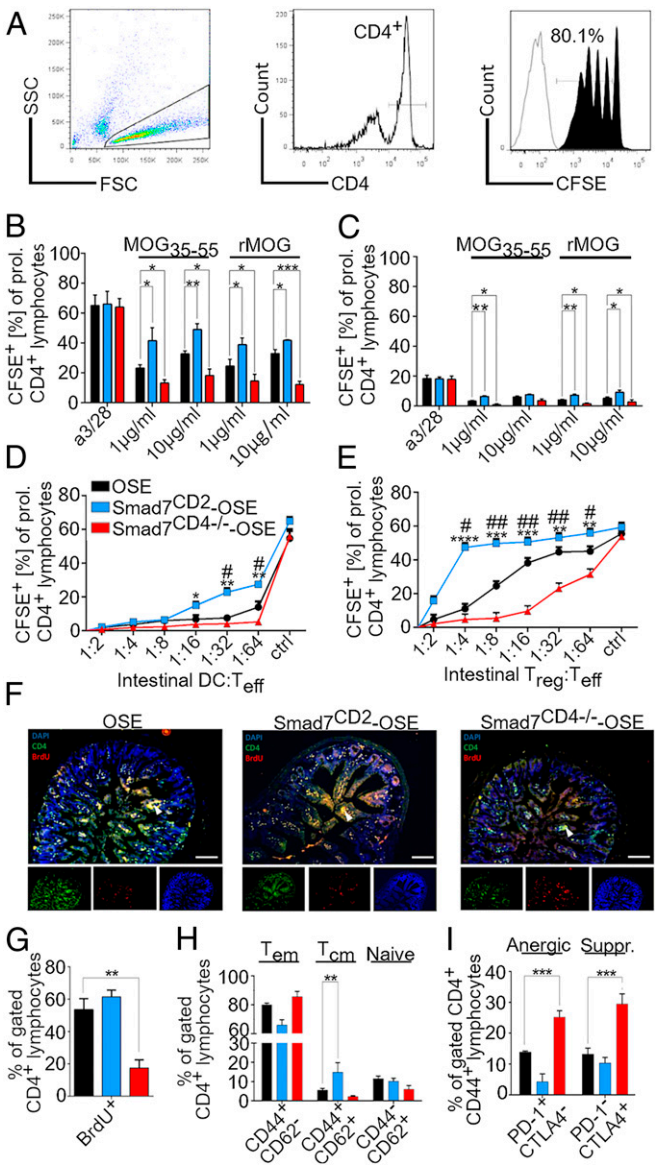

Fig. 3. Proliferation and tolerance of intestinal T cells are regulated by Smad7. (*A*) Gating strategy of proliferating lymphocytes upon 1 μg/mL $MOG_{35–55}$ restimulation. Shown is the gating of lymphocytes in the FSC and SSC; $CD4^+$ T cell divisions (black) are displayed in the histogram plot. (*B* and *C*) Proliferation analysis of $CD4^+$ T cells isolated from the lamina propria of the small and large intestine from 80-d-old OSE, $Smad7^{CD2}$-OSE, or $Smad7^{CD4-/-}$-OSE mice ($n = 12$ mice per group). Cells were stained with CFSE ex vivo and stimulated with 1 or 10 μg/mL $MOG_{35–55}$ and 1 or 10 μg/mL rMOG. (*D* and *E*) Suppression assay of lymph node-derived MOG-recognizing T effector cells from OSE, $Smad7^{CD2}$-OSE, or $Smad7^{CD4-/-}$-OSE mice, cocultured with intestinal dendritic cells and Tregs (both from wild-type mice). $MOG_{35–55}$ (10 μg/mL) and T cells were added simultaneously to stimulate T effector cells ($n = 4$ mice per group). (*F* and *G*) Eighty-day-old mice were analyzed by flow cytometry 24 h after BrdU injection for proliferation of T cells in the intestine ($n = 10$ mice each group). Slices were stained for $CD4^+$ T cells (green; *Left Insets*), proliferating cells (red; *Middle Insets*), and nuclei (blue; *Right Insets*). (*F*) Arrowheads indicate $CD4^+BrdU^+DAPI^+$ lymphocytes. (Scale bars, 200 μm.) (*H*) T cell analysis of central ($CD4^+CD44^+CD62L^-$) or effector-memory phenotype frequencies ($CD4^+CD44^+CD62L^+$) and of naïve T cell frequencies ($CD4^+CD44^-CD62L^+$) in the lamina propria ($n = 4$ mice each group). (*I*) Analysis of CD4, CD44, and either CTLA-4 or PD-1 to distinguish anergic T cells and Tregs obtained from the intestine ($n = 6$ mice each group). Data are shown as mean ± SEM. Statistical analyses were performed by 2-way ANOVA with Tukey post hoc test (*B*, *C*, and *G*–*I*). Suppression (*D* and *E*) was analyzed using 2-way ANOVA and Šidák post hoc test. $*P < 0.05$, $**P < 0.01$, $***P < 0.001$, $****P < 0.001$, $\#P < 0.05$, $\#\#P < 0.001$.

To understand the lack of proliferation in Smad7-deficient $CD4^+$ T cells, we analyzed $CD4^+CD44^+CD62^-$ (effector-memory) and $CD4^+CD44^+CD62^+$ (central-memory) T cells in the LP and found decreased numbers of effector-memory T cells and an increase of central-memory T cells in $Smad7^{CD2}$-OSE mice (Fig. 3*H*). Naïve $CD4^+CD44^-CD62^+$ T cells were unaltered between OSE, $Smad7^{CD2}$-OSE, and $Smad7^{CD4-/-}$-OSE mice.

Looking for suppressive mechanisms, we analyzed anergic T cells and tolerance-maintaining Tregs (35, 36) depending on TGF-β, which also includes type 1 regulatory (Tr1) T cells (37) as well as Th3 cells (38). We found increased numbers of $CD4^+CD44^+PD\text{-}1^+CTLA\text{-}4^-$ anergic T cells and $CD4^+CD44^+PD\text{-}1^-CTLA\text{-}4^+$ suppressive T cells in $Smad7^{CD4-/-}$-OSE mice (Fig. 3*I*).

In summary, these data show that Smad7 deletion in $CD4^+$ T cells favors the formation of suppressive T cells, for example Tregs, and anergic T cells in the intestinal mucosa, which potentially could protect mice from CNS autoimmunity.

Adoptively Transferred $CD4^+$ T Cells Primed in the Intestine Induce Experimental Autoimmune Encephalomyelitis Depending on Their Smad7 Expression. We hypothesized that intestinal $CD4^+$ T cells are required for the development of spontaneous autoimmune CNS demyelination, and that the intestine represents a site where those T cells are triggered and become autoreactive.

To establish a $MOG_{35–55}$–specific adoptive transfer (AT) EAE model, we first screened conditions with different genotypic combinations of $MOG_{35–55}$–specific $CD4^+$ T cells and recipient mice (*SI Appendix*, *Results*). Since all conditions with PTX treatment of recipient mice, irrespective of $MOG_{35–55}$ specificity, developed clinical symptoms (*SI Appendix*, Table S3, lines 1 to 4), we next developed a model lacking PTX treatment. We found that the TH genotype ($MOG_{35–55}$–specific B cells) for recipient mice and retinoic acid (RA) during in vitro $MOG_{35–55}$ restimulation are a requirement for induction of AT-EAE (*SI Appendix*, Table S3, lines 5 to 8). The vitamin A metabolite RA was used to up-regulate the gut-homing receptors CCR9 and α4β7 (39) on $CD4^+$ T cells (*SI Appendix*, Fig. S4*A*). While Th1 $CD4^+$ T cells responded very sparsely to RA stimulation, Tregs were very susceptible to RA ex vivo (*SI Appendix*, Fig. S4 *B*–*D*). RA has also been shown to influence T cell differentiation. While Th1 differentiation was unchanged between genotypes (*SI Appendix*, Fig. S4*E*), there was a trend toward diminished Th17 and to increased Treg differentiation under RA treatment (*SI Appendix*, Fig. S4 *F* and *G*).

Next, we performed various AT experiments with $MOG_{35–55}$–restimulated $CD4^+$ T cells obtained from sick OSE mice at day 80 of disease and transferred into healthy, 20-d-old OSE recipients. As a control, we first transferred lymph node-derived $CD4^+$ T cells from sick OSE mice, which led to AT-EAE in recipients only when these were treated with PTX (*SI Appendix*, Table S4, box A, lines 1 and 2). Treatment of lymph node-derived $CD4^+$ T cells from sick OSE mice with RA led to EAE in the absence of PTX treatment of recipients (*SI Appendix*, Table S4, box A, line 3). In contrast to lymph node-derived T cells, intestinally derived $CD4^+$ T cells caused AT-EAE in recipients also without additional injection of PTX (Fig. 4*A* and *SI Appendix*, Table S4, box A, lines 4 and 5). To investigate the contribution of Smad7 in T cells to AT-EAE, we used donor $CD4^+$ T cells from diseased OSE mice with either Smad7 overexpression or deletion. While intestinal $CD4^+$ T cells obtained from $Smad7^{CD2}$-OSE mice were able to induce AT-EAE in recipients without treatment of PTX, the transfer of intestinal $CD4^+$ T cells from $Smad^{CD4-/-}$-OSE mice did not induce AT-EAE (Fig. 4*A* and *SI Appendix*, Table S4, box A, lines 7 and 8).

To elucidate whether intestinal activation of $CD4^+$ T cells is required for disease induction, we treated $CD4^+$ T cells obtained from the lymph nodes and spleen of diseased $Smad7^{CD2}$-OSE mice with or without RA and transferred them to OSE recipient

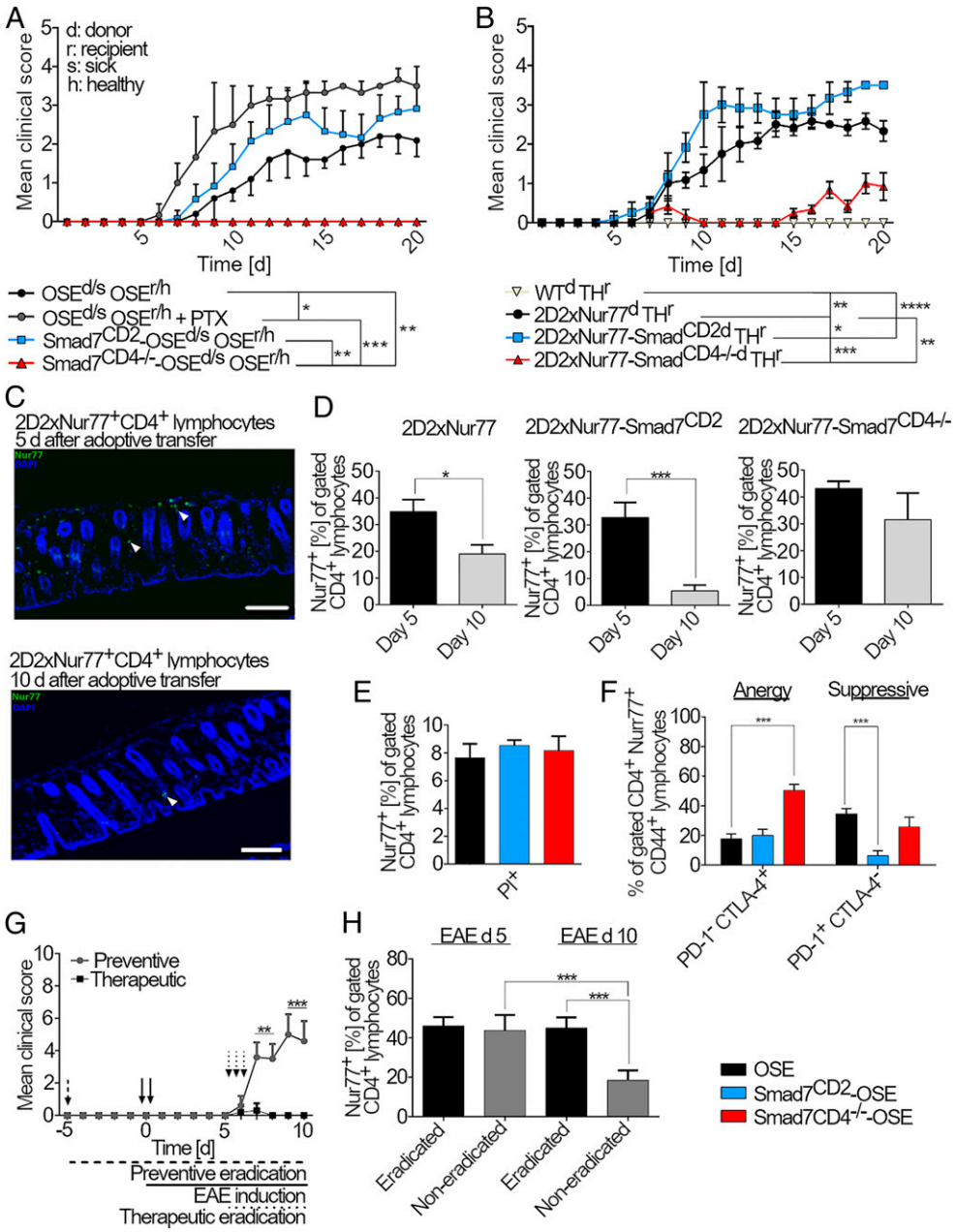

Fig. 4. Number of activated GFP-tagged T cells in the intestine at day 10 after adoptive transfer reciprocally correlates with clinical symptoms of adoptive transfer EAE. (*A*) $MOG_{35–55}$–recognizing $CD4^+$ T cells were obtained from the intestine from 80-d-old donor OSE, $Smad7^{CD2}$-OSE, or $Smad7^{CD4–/–}$-OSE mice with clinical disease. Isolated $CD4^+$ T cells were restimulated with 10 μg/mL $MOG_{35–55}$ for 24 h in vitro. In 1 experimental group, $CD4^+$ T cells additionally received retinoic acid for 24 h to up-regulate gut-homing receptors. Restimulated $CD4^+$ T cells (1×10^6) of the indicated genotype were injected i.p. into healthy 20-d-old OSE mice (recipients) to induce adoptive transfer EAE ($OSE^{don/sick}OSE^{rec/healthy}$, $n = 5$; $OSE^{don/sick}OSE^{rec/healthy}$ + PTX, $n = 3$; $Smad7^{CD2}$-$OSE^{don/sick}OSE^{rec/healthy}$, $n = 6$; $Smad7^{CD4–/–}OSE^{don/sick}OSE^{rec/healthy}$, $n = 3$). (*B*) 2D2 $CD4^+$ T cells were isolated from lymph nodes 30 d after immunization of donor wild-type (control), 2D2xNur77, 2D2xNur77-$Smad7^{CD2}$, or 2D2xNur77-$Smad7^{CD4–/–}$ mice with 10 μg/mL $MOG_{35–55}$. Nur77 was coupled with GFP as a reporter gene to track activated $CD4^+$ T cells. $CD4^+$ T cells were restimulated with 10 μg/mL $MOG_{35–55}$ and treated with 200 nM retinoic acid for 24 h in vitro. Restimulated $CD4^+$ T cells (1×10^6) of the indicated genotype were adoptively transferred into 20-d-old TH mice with $MOG^{35–55}$–specific B cells (recipients) to induce AT-EAE (WT^{don} in TH^{rec}, $n = 6$; 2D2xNur77^{don} in TH^{rec}, $n = 12$; 2D2xNur77-$Smad7^{CD2don}$ in TH^{rec}, $n = 12$; 2D2xNur77-$Smad7^{CD4–/–don}$ in TH^{rec}, $n = 12$). (*C*–*F*) $Nur77^+CD4^+$ T cells were isolated from lymph nodes 28 d after immunization with 10 μg/mL $MOG_{35–55}$, restimulated for 5 d with $MOG_{35–55}$ and RA, and adoptively transferred into TH mice. Mice were killed at day 5 or day 10. $Nur77^+CD4^+$ T cells were analyzed with histological staining (*C*) or $Nur77^+CD4^+$ T cells were isolated from the lamina propria and analyzed via flow cytometry (*D*–*F*). (*C* and *D*) Transferred $Nur77^+CD4^+$ T cells (arrow heads) were found in the lamina propria after 5 d (a representative picture from 2D2xNur77 ileum is shown in *C*). Transferred $Nur77^+CD4^+$ T cells vanished almost completely at day 10. Analysis of $Nur77^+CD4^+$ T cell number isolated from the LP 5 and 10 d after transfer is shown. (Scale bars, *C*, 200 μm.) (*E*) Frequencies of apoptotic lymphocytes from the LP 10 d after transfer of 2D2xNur77, 2D2xNur77-$Smad7^{CD2}$, and 2D2xNur77-$Smad7^{CD4–/–}$ $CD4^+$ T cells in TH mice. (*F*) Frequencies of $CD44^+$ and $PD\text{-}1^+$ (anergic) or $CTLA\text{-}4^+$ (Treg) intestinal $Nur77^+$ T cells. (*G*) The intestinal microbiota of recipient TH mice were eradicated 5 d prior to (↓) adoptive transfer of 2D2 $CD4^+$ T cells (↓↓) and mice were observed in order to investigate onset of clinical disease. In another experiment, therapeutic eradication of intestinal microbiota was performed when first clinical signs appeared (↓↓↓) ($n = 10$ each group). (*H*) Frequencies of transferred $CD4^+Nur77^+$ lymphocytes in the intestine of recipient TH mice at day 5 and 10. Data are shown as mean ± SEM. Statistical analysis for clinical disease course (*A* and *B*) was performed by AUC following a Mann–Whitney *U* test. Statistical analyses of the other experiments were performed by 2-way ANOVA with Šidák (*G*) or Tukey (*C*–*F* and *H*) post hoc test. $*P < 0.05$, $**P < 0.01$, $***P < 0.001$, $****P < 0.0001$.

mice. Only $CD4^+$ T cells that had received RA treatment to induce gut-homing receptors were able to induce AT-EAE in recipients (*SI Appendix*, Table S4, box A, lines 9 and 10).

These results indicate that up-regulation of gut-homing receptors in $CD4^+$ T cells has similar potency in inducing AT-EAE as the usage of intestinally derived $CD4^+$ T cells (as shown in Fig. 4*A*).

To address the question of whether 2D2 $CD4^+$ T cells with Smad7 overexpression or Smad7 deletion activated in the intestine can migrate to the CNS and cause inflammation, we took advantage of Nur77-expressing green fluorescent protein (GFP)-$CD4^+$ T cells for the AT as a reporter model (*SI Appendix*, Table S4, box B). GFP expression in $CD4^+$ T cells is induced during positive selection, requires MHC participation for maintenance, and directly correlates with the strength of the T cell receptor (TCR) stimulus (29). Nur77 mice were crossed with 2D2 mice for $MOG_{35–55}$ specificity (referred to as 2D2xNur77). Importantly, $CD4^+$ T cells in our experimental setup were treated with RA in vitro to induce intestinal homing by CCR9- and α4β7-dependent mechanisms. As a control, the transfer of wild type (WT)-derived $CD4^+$ T cells into TH mice did not induce AT-EAE without RA (Fig. 4*B* and *SI Appendix*, Table S4, box B, line 11).

2D2 and 2D2xNur77 $CD4^+$ T cells from lymph nodes and spleen were able to induce EAE in TH mice (Fig. 4*B* and *SI Appendix*, Table S4, box B, lines 12 and 13). Transfer of 2D2xNur77-Smad7^{CD2} $CD4^+$ T cells induced clinical signs after adoptive transfer into TH ($MOG_{35–55}$–specific B cells) recipients, while transfer of 2D2xNur77-Smad7$^{CD4–/–}$ $CD4^+$ T cells did not induce clinical signs (*SI Appendix*, Table S4, box B, lines 14 and 15). Hence, deletion of Smad7 in 2D2 $CD4^+$ T cells protects from AT-EAE while overexpression of Smad7 in 2D2 T cells worsens AT-EAE.

We used different time points after AT to track the migration of injected 2D2xNur77 $CD4^+$ T cells in recipients. Nur77 $CD4^+$ T cells isolated from spleen and lymph nodes could be observed in the intestine of TH ($MOG_{35–55}$–specific B cells) recipients at day 5 (Fig. 4*C*). T cells from 2D2xNur77 donors slightly, and from 2D2xNur77-Smad7^{CD2} donors almost completely, disappeared from the intestine at day 10 (Fig. 4 *C* and *D*). 2D2xNur77 and 2D2xNur77-Smad7$^{CD4–/–}$ T cells remained in the intestine throughout the evaluation time, which correlated with the absence of clinical signs (Fig. 4*D*).

To investigate the reason for the absence of clinical signs and stable frequencies of intestinal Nur77 $CD4^+$ T cells after transfer of 2D2xNur77-Smad7$^{CD4–/–}$ T cells, we investigated apoptosis and anergy of $CD4^+$ T cells. Apoptosis did not differ compared with 2D2xNur77 and 2D2xNur77-Smad7^{CD2} T cells (Fig. 4*E*). However, we observed elevated numbers of 2D2xNur77-Smad7$^{CD4–/–}$ T cells presenting with an anergic and suppressive phenotype (Fig. 4*F*). Regarding the influence of Smad7 overexpression on the function of Tregs, naïve $CD4^+$ T cells were differentiated under Treg conditions (*SI Appendix*, Fig. S4 *E–G*). We found less differentiation of Tregs as reported previously (10, 40). Measurement of the TGF-β and IL-10 secretion in the supernatant normalized to $CD4^+FoxP3^+$ T cells showed no differences between genotypes (*SI Appendix*, Fig. S4 *H* and *I*).

Eradication of the Microbiome Abolishes EAE Completely. To evaluate whether the gut microbiome is relevant for induction of CNS inflammation by gut-derived T cells, we treated mice with antibiotics 5 d before AT of 2D2xNur77 $CD4^+$ T cells in recipient mice. Indeed, the eradication of the microbiome abolished the development of disease completely (Fig. 4*G*). However, when we treated mice with antibiotics at a later time point, namely after EAE induction by $CD4^+$ T cell transfer, disease progressed unabated (Fig. 4*G*). The LP of treated mice at day 5 and day 10 had stable numbers of 2D2xNur77$^+$CD4$^+$ T cells, whereas noneradicated mice, which developed AT-EAE, had a significant decrease of 2D2xNur77$^+$CD4$^+$ T cells at day 10 (Fig. 4*H*).

We also performed additional AT experiments to block 2D2 $CD4^+$ T cell migration into the intestine. TR-14035 is known to specifically inhibit α4β7 on the cell surface (41). 2D2-, 2D2-Smad^{CD2}–, and 2D2-Smad7$^{CD4–/–}$–derived T cells were isolated and transferred into TH mice. Recipient mice were treated with 10 μM TR-14035 daily when T cells were transferred. Application of TR-14035 led to a potent amelioration of clinical signs of EAE, regardless of the genotype of transferred T cells (*SI Appendix*, Fig. S4 *J* and *K*). On the contrary, mice without TR-14035 treatment exhibited a more severe clinical EAE. Thus, blocking of the α4β7-chain attenuates AT-EAE.

We expected to find the transferred lymphocytes in the spinal cord (42). Indeed, 2D2xNur77 $CD4^+$ T cells were found in spinal cord lesions of diseased AT-EAE mice, with a clear increase when 2D2xNur77-Smad7^{CD2} $CD4^+$ T cells were transferred (Fig. 5*A*). Breakdown of the blood–brain barrier was markedly increased in recipient mice transferred with 2D2xNur77-Smad7^{CD2} $CD4^+$ T cells (*SI Appendix*, Fig. S5 *A* and *B*).

We investigated whether $CD4^+$ T cells in spinal cord infiltrations originated from the intestinal compartment depending on their genotype. While intestinal 2D2xNur77 and 2D2xNur77-Smad7$^{CD4–/–}$ $CD4^+$ T cells were close to absent, intestinal 2D2xNur77-Smad7^{CD2} $CD4^+$ T cells were found in high numbers in lesions of diseased mice (Fig. 5*B*). More than 40% of $CD4^+$ T cells in spinal cord lesions in the latter condition were Nur77$^+$ and originated from the intestine. As others have reported, most of the T cells in spinal cord lesions exhibit a Th17 phenotype (43), which was also found after transfer of 2D2xNur77 and 2D2xNur77-Smad7$^{CD4–/–}$ $CD4^+$ T cells (Fig. 5*C* and *SI Appendix*, Fig. S5*C*). In contrast, Smad7 overexpression in T cells led to enhanced occurrence of Th1 cells in CNS lesions, resulting in more severe damage of the spinal cord, accompanied by a reduced number of Treg cells, whereas after transfer of 2D2xNur77-Smad7$^{CD4–/–}$ $CD4^+$ T cells an increased frequency of Treg cells was found. Lesion-derived memory T cells consisted of T effector-memory cells (*SI Appendix*, Fig. S5*D*).

TGF-β–Dependent T Helper Cell Differentiation Is Altered in the Intestine of Multiple Sclerosis Patients. To evaluate whether Smad7 overexpression and alterations of T helper cell subsets are also found in the human intestine, we studied tissue samples from 27 MS and 27 control patients (*SI Appendix*, Fig. S6 and Table S1). We determined the expression levels of Smad7, the TGF-β downstream molecule pSmad2/3, and the T cell differentiation markers IL-17, FoxP3, and IFN-γ in the LP of terminal ileum- and colon-derived samples. The overall number of $CD4^+$ T cells did not differ between both groups (Fig. 6 and *SI Appendix*, Fig. S7). We found a trend toward increased frequencies of Smad7$^+$ cells in MS patients. Moreover, significantly more IFN-γ$^+$ cells were found in the LP of intestinal specimens from MS patients. Consistently, patients with MS showed significantly lower frequencies of pSmad2/3$^+$, FoxP3$^+$, and IL-17$^+$ cells.

Discussion

In this study, we examined the consequences of a reduced or increased expression of the TGF-β inhibitor Smad7 in T cells for experimental autoimmune CNS demyelination, and found that it is critical for disease induction at the intestinal barrier. We show that overexpression of Smad7 in T cells increases T cell activation, disease incidence, and severity in spontaneous OSE. Using adoptive transfer experiments, we demonstrate that $CD4^+$ T cells are induced at the intestinal mucosal barrier before migration to the CNS, depending on their Smad7 expression level. Eradication of the microbiome abolished disease induction. Deletion of Smad7 in T cells had a protective effect in the OSE model, due to a shift in the balance of T cell subsets toward an antiinflammatory and anergy-inducing phenotype. These animal experiments were corroborated by biopsies from MS patients, which showed a

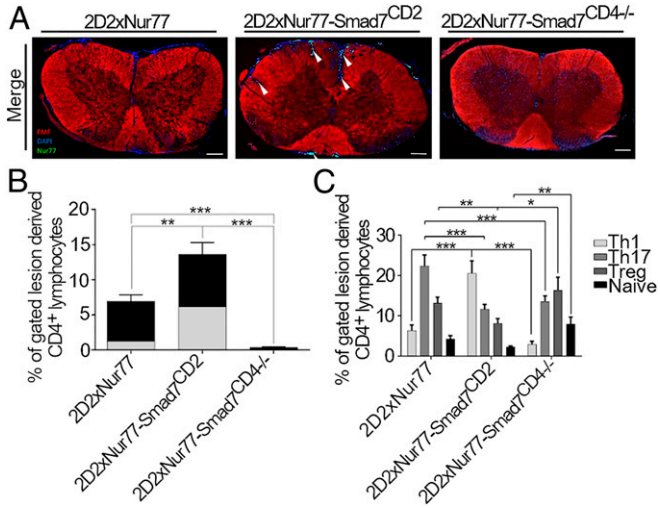

Fig. 5. 2D2xNur77 and 2D2xNur77-Smad7^{CD2} CD4$^+$ T cells accumulate in spinal cord lesions during AT-EAE. 2D2 CD4$^+$ T cells were isolated from lymph nodes of $MOG_{35–55}$–immunized donor 2D2xNur77, 2D2xNur77-Smad7^{CD2}, or 2D2xNur77-Smad7$^{CD4–/–}$ mice, restimulated with $MOG_{35–55}$ and 200 nM retinoic acid for 24 h, and adoptively transferred into 20-d-old TH mice (recipients) at 1×10^6 cells per transfer to induce AT-EAE. (*A*) Representative spinal cord sections of diseased recipient mice ($n = 6$ recipient mice per group). Slices were stained for FMF, DAPI, and GFP-tagged CD4$^+$ T cells. Light blue dots indicate GFP/DAPI double-positive Nur77-CD4$^+$ T cells (arrowhead). (Scale bars, 200 μm.) (*B*) Proportion of 2D2xNur77, 2D2xNur77-Smad7^{CD2}, or 2D2xNur77-Smad7$^{CD4–/–}$ CD4$^+$ T cells (gray) to the total number of isolated lymphocytes (black) from the spinal cord of recipient mice ($n = 6$ recipient mice per group). (*C*) Analysis of Th1, Th17, and Tregs of GFP-tagged, transferred CD4$^+$ T cell frequencies from the spinal cord of recipient mice ($n = 6$ recipient mice per group). Data are shown as mean ± SEM. Statistical analyses were performed by 2-way ANOVA with Tukey post hoc test. *$P < 0.05$, **$P < 0.01$, ***$P < 0.001$.

down-regulation of the TGF-β signaling molecule pSmad2/3, consistent with corresponding alterations of CD4$^+$ T cell differentiation markers in the intestinal LP. Our data indicate that Smad7 in T cells is an important inhibitor of tolerance mechanisms at the intestinal barrier, potentially contributing to the initiation of MS.

The pleiotropic cytokine TGF-β is an important regulator of immune responses, initiating signaling events in target cells that have vital and nonredundant regulatory functions (11). Although many immune cells are responsive to TGF-β, the loss of TGF-β signaling particularly in CD4$^+$ T cells, as shown in transgenic mice with a dominant-negative TGF-β receptor type II or with a specific deletion of the TGF-βR2 gene in T cells, results in the breakdown of tolerance and, consequently, autoimmunity. Paradoxically, chronic inflammation can persist in autoimmune diseases, despite increased local endogenous TGF-β expression (44). Smad7 expression is induced by proinflammatory cytokines like IFN-γ, TNF-α, and IL-1β (45), and thus inflammation itself might drive Smad7 expression and paralyze TGF-β signaling. Ex vivo suppression of Smad7 protein expression in mucosa-derived mononuclear cells or tissue cultures by specific antisense oligonucleotides both restores TGF-β signaling and decreases proinflammatory cytokine production (17, 46).

We have reported previously that an increased expression of the TGF-β inhibitor Smad7 in T cells worsens conventional EAE and increases T cell activation and differentiation toward Th1 cells, whereas Treg differentiation is decreased (10). Furthermore, we have found an up-regulation of Smad7 protein in lymph node cells upon restimulation with a CNS antigen (46) and of Smad7 mRNA in CD4$^+$ T cells from peripheral blood mononuclear cell (PBMC) samples of MS patients during acute relapses (10), suggesting an additional role of Smad7 during acute disease. In line with these findings, whole-genome transcription profiling of CD4$^+$ T lymphocytes from MS patients with acute relapse showed that treatment with i.v. methylprednisolone down-regulates Smad7 expression (47).

The adoptive transfer experiments with GFP-expressing CD4$^+$ T cells revealed that GFP$^+$CD4$^+$ T cells originating from the intestinal compartment contribute to CNS lesion formation, especially upon Smad7 overexpression. This, however, might be due to increased proliferation having more T cells patrolling and therefore encountering more MOG antigen in the CNS. Despite decreased numbers of Th17 cells in both Smad^{CD2}-OSE and Smad7$^{CD4–/–}$-OSE mice, we assume a differential mechanism in these genotypes. In Smad^{CD2}-OSE mice, the overexpression of Smad7 during T cell differentiation inhibits TGF-βR signaling and decreases numbers of Th17 cells and regulatory T cells (10, 40). TGF-β up-regulates RORγt and FoxP3, which can interact with each other. FoxP3 inhibits RORγt-mediated IL-17 gene interaction (48, 49). High concentrations of TGF-β result in increased levels of FoxP3 and induction of Tregs in the periphery. In contrast, low concentrations of TGF-β can synergize with inflammatory cytokines, such as IL-6, to increase differentiation of Th17 cells (48, 50). In Smad7CD4$^{–/–}$-OSE mice, we therefore assume that increased TGF-β signaling leads to Treg differentiation, consequently suppressing Th17 generation.

There is a comorbidity of MS with inflammatory bowel disease (51), and white matter lesions are common in the latter. Inflammatory bowel disease is associated with breakdown of the intestinal barrier and Smad7 is overexpressed in mucosal lesions, leading to a blockade of TGF-β signaling and a disturbed homeostasis of T cell subsets toward inflammatory phenotypes (17, 44). Similar to this situation, we found a trend toward an increase of Smad7 in accordance with significantly decreased pSmad2/3 in the intestinal mucosa of MS patients, indicating a dysfunctional TGF-β signaling. Corresponding alterations of T helper cell subsets were detected, with an increase of the inflammatory Th1 marker IFN-γ and decrease of the antiinflammatory Treg marker FoxP3. Our results are in line with a recent investigation showing a decrease in the number of CD4$^+$CD25$^+$CD127$^–$ Treg cells in the distal colon of patients with early MS (52). Epithelial cells, myeloid cells, and lymphocytes of the intestinal mucosa secrete

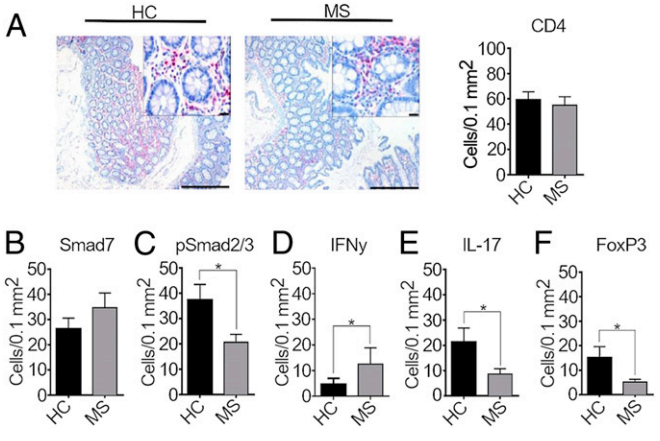

Fig. 6. Altered T cell subset occurrence in the lamina propria of patients with multiple sclerosis. Comparison of markers for TGF-β signaling and T cell differentiation in intestinal biopsies from patients with relapsing or progressive MS ($n = 27$) and healthy controls (HC; $n = 27$). (*A*) Comparison of the occurrence of CD4$^+$ T cells in MS samples or HC. (Scale bars, 500 and 100 μm [*Insets*].) (*B* and *C*) Analysis of the TGF-β inhibitor Smad7 and the TGF-β signaling pathway molecule pSmad2/3. (*D–F*) Cytokine analysis of IFN-γ, IL-17, and FoxP3. Data are shown as mean ± SEM. Statistical analyses were performed with Student's *t* test in case data were normally distributed and Mann–Whitney *U* test in case data were not normally distributed. *$P < 0.05$.

TGF-β, which acts both in a paracrine and autocrine fashion to maintain intestinal integrity and immune homeostasis in the microbe- and antigen-rich environment of the gut (53). Activation of the TGF-β pathway and synergism with immunoregulatory factors such as RA strengthen immunosuppression toward commensal microbes and innocuous food antigens.

The intestinal barrier has received increasing attention as an important site for the interaction of the luminal microbiome and the host in MS patients (54). Microbial colonization of the intestine is mandatory for the initiation of CNS-directed inflammation and consecutive demyelination in the OSE model (55). A recent case report identified highly conserved intestinal $CD4^+$ T cell receptors on mucosal associated invariant T cells in a post mortem brain analysis of an MS patient (56), indicating contribution of intestinal T cell subsets in the pathophysiology of MS. This is in line with our preclinical data, which demonstrated that treatment of $CD4^+$ T cells with RA to force activation at the mucosal barrier was mandatory to initiate CNS inflammation. Indeed, antibiotic treatment of EAE mice reduces the frequency of intestinally derived $CCR9^+CD4^+$ memory lymphocytes in the blood, leading to an amelioration of EAE. $CCR9^+CD4^+$ memory lymphocytes found in the CSF of SPMS patients exhibit a proinflammatory, IFN-γ and IL-17 secreting profile (57). Intestinal resident LAG-3^+ IELs, characterized by a Th17-like profile, are known to invade the CNS (6). Signaling of resident LAG-3^+ IELs depends on dietary aryl hydrocarbon receptor ligands (6), a possible target for further investigation in the context of Smad7 interaction. Other studies discussed the influence of follicular T helper (Tfh) cells on infiltrating B cells during the peak of Th17-related EAE induction. Tfh cells are capable of inducing EAE in the AT model by contributing to inflammatory B cell responses (58). In Lewis rats, T cells are primed in the lung to enter the CNS, causing inflammation (8). Whether these T cells are also migrating to the intestinal compartment and whether inflammatory lesion-derived B cells contribute to the pathogenesis of OSE need to be determined in future experiments.

We also addressed the question of whether Smad7 expression in $CD4^+$ T cells might facilitate breakdown of the blood–brain barrier. Our adoptive transfer experiments suggested that the interaction of MOG-recognizing B cells and Smad7-overexpressing, MOG-recognizing T cells is mandatory to induce blood–brain barrier leakage and CNS migration of $CD4^+$ T cells. This is crucial, since for induction of conventional EAE, pertussis toxin is needed to induce blood–brain barrier disruption. This could be related to the release of proinflammatory cytokines or cell-surface markers by Smad7-overexpressing T cells (59). Ig isotype switching is critically mediated by activated T cells via transient expression of CD40 ligand (CD40L) and production of cytokines such as IL-4 or IL-13 (60). Increased numbers of Th1 cells, in particular the secretion of the Th1-dependent IFN-γ, induce an isotype switch into IgG2 immune globulins in B cells (61–63). Another recent study revealed that IgA^+ plasma cells from the intestine are capable of migration into the CNS and attenuate EAE clinical signs via IL-10 secretion (64).

There are various approaches to modulate the intestinal immune system, such as treatment with short-chain fatty acids, which increases lamina propria-derived Treg cells (7), or with a probiotic mixture containing *Lactobacillus*, *Bifidobacterium*, and *Streptococcus*, which changes the composition of gut microbiota and induces an antiinflammatory immune phenotype in the blood of MS patients (65). Some commensal microbes also reduce the expression level of Smad7 in vivo in human PBMCs (66) or in vitro in intestinal epithelial cells (67, 68). Another approach developed for inflammatory bowel diseases, such as Crohn's disease and ulcerative colitis, is to target increased Smad7 expression in the intestine. The oral Smad7 antisense molecule Mongersen reached 58% (40 mg) and 72% (160 mg) clinical response in Crohn's disease, compared with 17% of placebo in a phase II trial (18), but failed significance in an interim analysis of a phase III clinical trial and was therefore stopped. Nevertheless, Smad7 inhibition could be an interesting avenue in MS therapy due to the aforementioned benefitial effects on lymphocyte subsets and tolerance mechanisms.

There are several limitations of our study. First, our experiments rely on the OSE model, characterized by autoreactivity of T and B cells against MOG. The occurrence of a single MOG-specific TCR in T and B cells is not seen in MS patients. The OSE model represents a cross-over model with pathogenic features of both neuromyelitis optica and MS. Smad7 overexpression in $CD4^+$ T cells in our model is permanent due to gene expression under control of the CD2 promotor; hence, negative feedback loops via TGF-β are permanently shut down in T cells, a situation which probably is only found in phases of active disease during MS (10). Moreover, several lymphocyte subsets and interesting pathways were not pursued in this study but should be addressed in further experiments, such as the role of B cells, the incomplete inhibition of $CD4^+$ T cell migration to the intestinal compartment via blocking the α4β7-chain by additional inhibition of the CCR9 receptor (41), and the contribution of $CD8^+$ T cells (69). Another limitation is the small number of biopsy samples from MS patients. Due to technical reasons, we were not able to costain for CD4 in these biopsy samples. In addition, changes of the composition of intestinal IFN-γ^+ versus regulatory T cells might not exclusively be due to MS, since patients underwent colonoscopy also for other indications. Most human biopsy samples in this retrospective series were obtained from the colon, whereas rodent data suggest that dysregulation of Smad7 is mostly found in the terminal ileum. Another limitation of our study is that we did not evaluate whether Smad7 modification is also associated with changes of the microbiome. These investigations were outside the scope of the current project, but should be addressed in future studies.

In summary, we show that Smad7 is critically involved in the priming of intestinal autoreactive $CD4^+$ T cells and migration of these cells to the CNS with consecutive inflammation and demyelination. We describe that Smad7 expression in T cells itself does not cause clinical signs but increases the autoreactive capacity of pathogenic T cells and breakdown of suppressive mechanisms at the intestinal barrier. The inhibition of Smad7 in intestinal lymphocytes by pharmaceuticals or dietary components might reduce antigen susceptibility of autoreactive T cells in the intestine, decrease local inflammation and initiation of autoimmunity, and finally prevent further disease activity in MS.

ACKNOWLEDGMENTS. IgH^{MOG} mice were kindly provided by Gurumoorthy Krishnamoorthy, Max Planck Institute of Biochemistry, Martinsried, and Luisa Klotz, Department of Neurology, University of Münster. This study was supported by grants from the German Research Council (KL2187/1-1) and FoRUM (F758II-2013) (both to I.K.).

1. J. M. Allaire *et al*., The intestinal epithelium: Central coordinator of mucosal immunity. *Trends Immunol.* **39**, 677–696 (2018).
2. K. Berer *et al*., Commensal microbiota and myelin autoantigen cooperate to trigger autoimmune demyelination. *Nature* **479**, 538–541 (2011).
3. E. Cekanaviciute *et al*., Gut bacteria from multiple sclerosis patients modulate human T cells and exacerbate symptoms in mouse models. *Proc. Natl. Acad. Sci. U.S.A.* **114**, 10713–10718 (2017).
4. A. J. Thompson, S. E. Baranzini, J. Geurts, B. Hemmer, O. Ciccarelli, Multiple sclerosis. *Lancet* **391**, 1622–1636 (2018).
5. R. Hohlfeld, K. Dornmair, E. Meinl, H. Wekerle, The search for the target antigens of multiple sclerosis, part 1: Autoreactive $CD4^+$ T lymphocytes as pathogenic effectors and therapeutic targets. *Lancet Neurol.* **15**, 198–209 (2016).
6. A. Kadowaki *et al*., Gut environment-induced intraepithelial autoreactive CD4(+) T cells suppress central nervous system autoimmunity via LAG-3. *Nat. Commun.* **7**, 11639 (2016).
7. A. Haghikia *et al*., Dietary fatty acids directly impact central nervous system autoimmunity via the small intestine. *Immunity* **43**, 817–829 (2015).
8. F. Odoardi *et al*., T cells become licensed in the lung to enter the central nervous system. *Nature* **488**, 675–679 (2012).

9. J. Breuer *et al*., Ultraviolet B light attenuates the systemic immune response in central nervous system autoimmunity. *Ann. Neurol.* **75**, 739–758 (2014).
10. I. Kleiter *et al*., Smad7 in T cells drives T helper 1 responses in multiple sclerosis and experimental autoimmune encephalomyelitis. *Brain* **133**, 1067–1081 (2010).
11. W. Chen, P. Ten Dijke, Immunoregulation by members of the TGFβ superfamily. *Nat. Rev. Immunol.* **16**, 723–740 (2016).
12. M. C. Fantini *et al*., Cutting edge: TGF-beta induces a regulatory phenotype in $CD4^+$ $CD25^-$ T cells through Foxp3 induction and down-regulation of Smad7. *J. Immunol.* **172**, 5149–5153 (2004).
13. P. R. Mangan *et al*., Transforming growth factor-beta induces development of the T(H)17 lineage. *Nature* **441**, 231–234 (2006).
14. M. Veldhoen, R. J. Hocking, C. J. Atkins, R. M. Locksley, B. Stockinger, TGFbeta in the context of an inflammatory cytokine milieu supports de novo differentiation of IL-17-producing T cells. *Immunity* **24**, 179–189 (2006).
15. L. Gorelik, P. E. Fields, R. A. Flavell, Cutting edge: TGF-beta inhibits Th type 2 development through inhibition of GATA-3 expression. *J. Immunol.* **165**, 4773–4777 (2000).
16. L. Gorelik, S. Constant, R. A. Flavell, Mechanism of transforming growth factor beta-induced inhibition of T helper type 1 differentiation. *J. Exp. Med.* **195**, 1499–1505 (2002).
17. G. Monteleone *et al*., Blocking Smad7 restores TGF-beta1 signaling in chronic inflammatory bowel disease. *J. Clin. Invest.* **108**, 601–609 (2001).
18. G. Monteleone *et al*., Mongersen, an oral SMAD7 antisense oligonucleotide, and Crohn's disease. *N. Engl. J. Med.* **372**, 1104–1113 (2015).
19. S. El Aidy, T. G. Dinan, J. F. Cryan, Immune modulation of the brain-gut-microbe axis. *Front. Microbiol.* **5**, 146 (2014).
20. N. Powell, M. M. Walker, N. J. Talley, The mucosal immune system: Master regulator of bidirectional gut-brain communications. *Nat. Rev. Gastroenterol. Hepatol.* **14**, 143–159 (2017).
21. J. E. Libbey, M. F. Cusick, R. S. Fujinami, Role of pathogens in multiple sclerosis. *Int. Rev. Immunol.* **33**, 266–283 (2014).
22. S. Miyake, T. Yamamura, Gut environmental factors and multiple sclerosis. *J. Neuroimmunol.* **329**, 20–23 (2019).
23. M. Sun, C. He, Y. Cong, Z. Liu, Regulatory immune cells in regulation of intestinal inflammatory response to microbiota. *Mucosal Immunol.* **8**, 969–978 (2015).
24. G. Krishnamoorthy, H. Lassmann, H. Wekerle, A. Holz, Spontaneous opticospinal encephalomyelitis in a double-transgenic mouse model of autoimmune T cell/B cell cooperation. *J. Clin. Invest.* **116**, 2385–2392 (2006).
25. E. Bettelli, D. Baeten, A. Jäger, R. A. Sobel, V. K. Kuchroo, Myelin oligodendrocyte glycoprotein-specific T and B cells cooperate to induce a Devic-like disease in mice. *J. Clin. Invest.* **116**, 2393–2402 (2006).
26. E. Bettelli *et al*., Myelin oligodendrocyte glycoprotein-specific T cell receptor transgenic mice develop spontaneous autoimmune optic neuritis. *J. Exp. Med.* **197**, 1073–1081 (2003).
27. T. Litzenburger *et al*., B lymphocytes producing demyelinating autoantibodies: Development and function in gene-targeted transgenic mice. *J. Exp. Med.* **188**, 169–180 (1998).
28. S. Dominitzki *et al*., Cutting edge: *Trans*-signaling via the soluble IL-6R abrogates the induction of FoxP3 in naive $CD4^+CD25$ T cells. *J. Immunol.* **179**, 2041–2045 (2007).
29. A. E. Moran *et al*., T cell receptor signal strength in Treg and iNKT cell development demonstrated by a novel fluorescent reporter mouse. *J. Exp. Med.* **208**, 1279–1289 (2011).
30. I. Ayzenberg *et al*., Analysis of neurogenesis during experimental autoimmune encephalomyelitis reveals pitfalls of bioluminescence imaging. *PLoS One* **10**, e0118550 (2015).
31. D. P. McCarthy, M. H. Richards, S. D. Miller, Mouse models of multiple sclerosis: Experimental autoimmune encephalomyelitis and Theiler's virus-induced demyelinating disease. *Methods Mol. Biol.* **900**, 381–401 (2012).
32. P. D. Cravens *et al*., Lymph node-derived donor encephalitogenic $CD4^+$ T cells in C57BL/6 mice adoptive transfer experimental autoimmune encephalomyelitis highly express GM-CSF and T-bet. *J. Neuroinflammation* **8**, 73 (2011).
33. J. Ochoa-Repáraz *et al*., Role of gut commensal microflora in the development of experimental autoimmune encephalomyelitis. *J. Immunol.* **183**, 6041–6050 (2009).
34. J. Cortijo *et al*., A small molecule, orally active, alpha4beta1/alpha4beta7 dual antagonist reduces leukocyte infiltration and airway hyper-responsiveness in an experimental model of allergic asthma in brown Norway rats. *Br. J. Pharmacol.* **147**, 661–670 (2006).
35. R. H. Friedline *et al*., $CD4^+$ regulatory T cells require CTLA-4 for the maintenance of systemic tolerance. *J. Exp. Med.* **206**, 421–434 (2009).
36. L. A. Kalekar *et al*., CD4(+) T cell anergy prevents autoimmunity and generates regulatory T cell precursors. *Nat. Immunol.* **17**, 304–314 (2016).
37. A. M. White, D. C. Wraith, Tr1-like T cells—An enigmatic regulatory T cell lineage. *Front. Immunol.* **7**, 355 (2016).
38. Y. Chen, V. K. Kuchroo, J. Inobe, D. A. Hafler, H. L. Weiner, Regulatory T cell clones induced by oral tolerance: Suppression of autoimmune encephalomyelitis. *Science* **265**, 1237–1240 (1994).
39. E. J. Villablanca, J. R. Mora, Competitive homing assays to study gut-tropic T cell migration. *J. Vis. Exp.* ((49):), 2619 (2011).
40. M. Hasan *et al*., Activation of TGF-β-induced non-Smad signaling pathways during Th17 differentiation. *Immunol. Cell Biol.* **93**, 662–672 (2015).
41. L. A. Egger *et al*., Alpha(4)beta(7)/alpha(4)beta(1) dual integrin antagonists block alpha(4)beta(7)-dependent adhesion under shear flow. *J. Pharmacol. Exp. Ther.* **302**, 153–162 (2002).
42. S. D. Miller, W. J. Karpus, Experimental autoimmune encephalomyelitis in the mouse. *Curr. Protoc. Immunol.* **77**, 15.1.1–15.1.18 (2007).
43. D. J. Cua *et al*., Interleukin-23 rather than interleukin-12 is the critical cytokine for autoimmune inflammation of the brain. *Nature* **421**, 744–748 (2003).
44. G. Monteleone *et al*., A failure of transforming growth factor-beta1 negative regulation maintains sustained NF-kappaB activation in gut inflammation. *J. Biol. Chem.* **279**, 3925–3932 (2004).
45. L. Ulloa, J. Doody, J. Massagué, Inhibition of transforming growth factor-beta/SMAD signalling by the interferon-gamma/STAT pathway. *Nature* **397**, 710–713 (1999).
46. I. Kleiter *et al*., Inhibition of Smad7, a negative regulator of TGF-beta signaling, suppresses autoimmune encephalomyelitis. *J. Neuroimmunol.* **187**, 61–73 (2007).
47. C. De Andres *et al*., Genes differentially expressed by methylprednisolone in vivo in CD4 T lymphocytes from multiple sclerosis patients: Potential biomarkers. *Pharmacogenomics J.* **18**, 98–105 (2018).
48. L. Zhou *et al*., TGF-beta-induced Foxp3 inhibits T(H)17 cell differentiation by antagonizing RORgammat function. *Nature* **453**, 236–240 (2008).
49. K. Ichiyama *et al*., Foxp3 inhibits RORgammat-mediated IL-17A mRNA transcription through direct interaction with RORgammat. *J. Biol. Chem.* **283**, 17003–17008 (2008).
50. R. Basu, R. D. Hatton, C. T. Weaver, The Th17 family: Flexibility follows function. *Immunol. Rev.* **252**, 89–103 (2013).
51. M. Kosmidou *et al*., Multiple sclerosis and inflammatory bowel diseases: A systematic review and meta-analysis. *J. Neurol.* **264**, 254–259 (2017).
52. A. M. Moser *et al*., Mucosal biopsy shows immunologic changes of the colon in patients with early MS. *Neurol. Neuroimmunol. Neuroinflamm.* **4**, e362 (2017).
53. N. Malhotra, J. Kang, SMAD regulatory networks construct a balanced immune system. *Immunology* **139**, 1–10 (2013).
54. C. R. Camara-Lemarroy, L. Metz, J. B. Meddings, K. A. Sharkey, V. Wee Yong, The intestinal barrier in multiple sclerosis: Implications for pathophysiology and therapeutics. *Brain* **141**, 1900–1916 (2018).
55. K. Berer *et al*., Gut microbiota from multiple sclerosis patients enables spontaneous autoimmune encephalomyelitis in mice. *Proc. Natl. Acad. Sci. U.S.A.* **114**, 10719–10724 (2017).
56. K. Held *et al*., αβ T-cell receptors from multiple sclerosis brain lesions show MAIT cell-related features. *Neurol. Neuroimmunol. Neuroinflamm.* **2**, e107 (2015).
57. A. Kadowaki, R. Saga, Y. Lin, W. Sato, T. Yamamura, Gut microbiota-dependent $CCR9^+CD4^+$ T cells are altered in secondary progressive multiple sclerosis. *Brain* **142**, 916–931 (2019).
58. J. L. Quinn, G. Kumar, A. Agasing, R. M. Ko, R. C. Axtell, Role of TFH cells in promoting T helper 17-induced neuroinflammation. *Front. Immunol.* **9**, 382 (2018).
59. W. Pan *et al*., Cytokine signaling modulates blood-brain barrier function. *Curr. Pharm. Des.* **17**, 3729–3740 (2011).
60. S. G. Tangye, A. Ferguson, D. T. Avery, C. S. Ma, P. D. Hodgkin, Isotype switching by human B cells is division-associated and regulated by cytokines. *J. Immunol.* **169**, 4298–4306 (2002).
61. S. Huang *et al*., Immune response in mice that lack the interferon-gamma receptor. *Science* **259**, 1742–1745 (1993).
62. C. M. Snapper, C. Peschel, W. E. Paul, IFN-gamma stimulates IgG2a secretion by murine B cells stimulated with bacterial lipopolysaccharide. *J. Immunol.* **140**, 2121–2127 (1988).
63. K. M. Smith *et al*., Th1 and Th2 $CD4^+$ T cells provide help for B cell clonal expansion and antibody synthesis in a similar manner in vivo. *J. Immunol.* **165**, 3136–3144 (2000).
64. O. L. Rojas *et al*., Recirculating intestinal IgA-producing cells regulate neuroinflammation via IL-10. *Cell* **176**, 610–624.e18 (2019).
65. S. K. Tankou *et al*., A probiotic modulates the microbiome and immunity in multiple sclerosis. *Ann. Neurol.* **83**, 1147–1161 (2018).
66. T. Fujii *et al*., *Bifidobacterium breve* enhances transforming growth factor beta1 signaling by regulating Smad7 expression in preterm infants. *J. Pediatr. Gastroenterol. Nutr.* **43**, 83–88 (2006).
67. O. T. Foye, I. F. Huang, C. C. Chiou, W. A. Walker, H. N. Shi, Early administration of probiotic *Lactobacillus acidophilus* and/or prebiotic inulin attenuates pathogen-mediated intestinal inflammation and Smad 7 cell signaling. *FEMS Immunol. Med. Microbiol.* **65**, 467–480 (2012).
68. Y. J. Yang, C. C. Chuang, H. B. Yang, C. C. Lu, B. S. Sheu, *Lactobacillus acidophilus* ameliorates *H. pylori*-induced gastric inflammation by inactivating the Smad7 and NFκB pathways. *BMC Microbiol.* **12**, 38 (2012).
69. S. Sinha, A. W. Boyden, F. R. Itani, M. P. Crawford, N. J. Karandikar, CD8(+) T-cells as immune regulators of multiple sclerosis. *Front. Immunol.* **6**, 619 (2015).